Thermodynamic Properties of Toluene Solutions of Low Molecular Weight Polystyrenes over Wide Ranges of Concentration

Ryohei Koyama and Takahiro Sato*

Department of Macromolecular Science, Osaka University, 1-1 Machikaneyama-cho, Toyonaka, Osaka 560-0043, Japan

Received August 28, 2001; Revised Manuscript Received December 12, 2001

ABSTRACT: Second and third virial coefficients, A_2 and A_3, as well as the reciprocal of the osmotic compressibility $\partial\Pi/\partial c$ up to high concentrations were measured for low molecular weight polystyrenes dissolved in a good solvent toluene, by sedimentation equilibrium. The results were compared with a theory based on the single-contact approximation, where the polymer chain is viewed as a spherocylinder bearing hard-core and square-well potentials, to determine the hard-core diameter and the depth of the square-well potential of polystyrene in toluene. Furthermore, the present results of A_2, A_3, and $\partial\Pi/\partial c$ were combined with previous ones for higher molecular weight polystyrenes in toluene to examine application limits of the single-contact approximation. It was found that $\partial\Pi/\partial c$ for a polymer concentration higher than ca. 0.1 g/cm^3 is described by the theory of the single-contact approximation, irrespective of the polystyrene molecular weight, indicating that the effect of multiple contacts on $\partial\Pi/\partial c$ is screening off in the concentrated region.

1. Introduction

Solutions of flexible polymers dissolved in good solvents are often divided into three concentration regions: dilute, semidilute, and concentrated.[1−3] In each concentration region, thermodynamic properties of the solutions show characteristic concentration and molecular weight dependences and are discussed in different theoretical framework.

For dilute solutions, thermodynamic properties are expressed in the form of the virial expansion, and molecular weight dependences of the second and third virial coefficients (A_2 and A_3, respectively) are the main problems in this region. Enormous efforts have been made to these problems.[3−6] Thermodynamic properties of semidilute solutions are known to show characteristic universality, and their concentration and molecular weight dependences can be expressed in terms of a single scaling parameter c/c^*, where c is the polymer mass concentration and c^* is the overlap concentration depending on the molecular weight.[1−3] Since the mean-field approximation is not applicable to this region, the scaling function has been formulated by renormalization group theories.[7,8] In the concentrated region, the finite size of the monomer unit of polymer chains becomes important, and the universality in semidilute solutions breaks down. As a result, thermodynamic functions are no more expressed by the scaling parameter c/c^*. However, the density fluctuation of monomer units diminishes in this region, so that the mean-field approximation becomes applicable. Thermodynamic properties of concentrated solutions are often argued by using the classical Flory−Huggins theory[9] with the phenomenological χ parameter.

When the polymer molecular weight is decreased, the above scheme of the three concentration regions must be modified. With decreasing molecular weight, the crossover concentration (equal to c^*) between the dilute and semidilute regions increases but that between the semidilute and concentrated regions stays constant, so that the semidilute region becomes narrow and finally disappears. Noda et al.[10] reported that the two crossover concentrations merge at a molecular weight of few tens of thousands for the polystyrene−toluene system.

The lowering of the polymer molecular weight also essentially affects dilute solution properties. For flexible polymers modeled as Gaussian chains, A_2 and A_3 are expressed in infinite power series of the excluded-volume parameter, and the convergence of the series is rather poor in good solvents at a high degree of polymerization.[4,6] On the other hand, as demonstrated by Yamakawa et al.,[6] the chain stiffness effect becomes appreciable even for flexible polymers in a low molecular weight region, so that we may expect that the probability of simultaneous contacts of two polymer chains at two or more different portions diminishes. As a result, the second- and higher-order perturbation terms in the series, called the multiple-contact terms, are expected to become less important than the first-order term, which is the *single-contact term*, as in the case of stiff or semiflexible polymer solutions.[11]

In the present work, we investigated thermodynamic properties of toluene solutions of low molecular weight polystyrenes over wide ranges of the polymer concentration by sedimentation equilibrium. Although thermodynamic properties of the polystyrene−toluene system have been already studied by many workers,[10,12−17] there have been no reports on the system in a low molecular weight range of polymers and over wide concentration ranges from dilute through concentrated, to our best knowledge. In this paper, A_2 and A_3 as well as the reciprocal of the osmotic compressibility $\partial\Pi/\partial c$ up to high concentrations obtained experimentally are compared with a theory based on the single-contact approximation (cf. section 2), where the polymer chain is viewed as a spherocylinder bearing hard-core and square-well attractive potentials, to determine the hard-core diameter and the depth of the square-well potential of polystyrene in toluene. Furthermore, the limit of the applicability of the single-contact approximation is discussed by combining the present and previous data of A_2, A_3, and $\partial\Pi/\partial c$.

10.1021/ma011540z CCC: $22.00
Published on Web 02/16/2002

2. Theoretical Section

Single-Contact Approximation To Formulate $\partial\Pi/\partial c$. For two rodlike polymer chains (not in the parallel configuration), we can define a pair of the closest approaching contour points on the two chains, and the intermolecular interaction potential $u(r)$ can be written as a function of the distance r between the closest approaching contour points. Even for flexible polymers, if the probability of multiple contacts is negligible, we may use the same $u(r)$ for the potential between two polymer chains in a good approximation. In what follows, we use this single-contact approximation.

The intermolecular interaction between neutral polymer chains consists of the harshly repulsive and soft attractive (the dispersion) interactions. Considering the polymer-chain end effect on the latter interaction, we may write $u(r)$ as

$$u(r) = u_0(r) + w_{mm}(r) + w_{me}(r) + w_{ee}(r) \quad (2.1)$$

where $u_0(r)$ is the repulsive potential, and $w_{mm}(r)$, $w_{me}(r)$, and $w_{ee}(r)$ are dispersion potentials between chain middle portions, between middle and end portions, and between chain end portions, respectively. If $u_0(r)$ is chosen as the reference potential and the remaining potentials are treated as thermodynamic perturbations,[18,19] the excess free energy ΔF of the polymer solution over that of the solvent may be given by

$$\Delta F = \Delta F_0 + \Delta F_{w,mm} + \Delta F_{w,me} + \Delta F_{w,ee} \quad (2.2)$$

where ΔF_0 is ΔF for the reference system with $u(r) = u_0(r)$ and where $\Delta F_{w,mm}$, $\Delta F_{w,me}$, and $\Delta F_{w,ee}$ are perturbation terms corresponding to the potentials $w_{mm}(r)$, $w_{me}(r)$, and $w_{ee}(r)$.

If the harshly repulsive potential $u_0(r)$ is approximated by the hard-core potential, ΔF_0 may be formulated by the scaled particle theory for the hard spherocylinder system, for which the result is written as[20]

$$\frac{\Delta F_0}{nk_BT} = \frac{\mu^\circ}{k_BT} - 1 + \ln\left(\frac{c'}{1-vc'}\right) + \frac{B}{2}\left(\frac{c'}{1-vc'}\right) + \frac{C}{3}\left(\frac{c'}{1-vc'}\right)^2 + \sigma \quad (2.3)$$

where n, v, μ°, and c' are the number, the volume, the standard chemical potential, and the number concentration of spherocylinders in solution, respectively, and k_BT is the Boltzmann constant multiplied by the absolute temperature. The coefficients B and C are defined by

$$B = \frac{\pi}{4}{L_c}^2 d\rho + 6v, \quad C = \left(v + \frac{\pi}{12}d^3\right)\left(B - 2v - \frac{\pi}{6}d^3\right) \quad (2.4)$$

where d and L_c are the hard-core diameter and the contour length of the cylinder part of the spherocylinder, respectively, and ρ is an orientation-dependent parameter defined by

$$\rho \equiv \frac{4}{\pi}\int\int d\mathbf{a}_1\, d\mathbf{a}_2 |\mathbf{a}_1 \times \mathbf{a}_2| \bar{f}(\mathbf{a}_1)\bar{f}(\mathbf{a}_2) \quad (2.5)$$

Here $\mathbf{a}_1$ and $\mathbf{a}_2$ are the unit tangent vectors to the closest approaching contour points on two interacting chains 1 and 2, and $\bar{f}(\mathbf{a}_1)$ and $\bar{f}(\mathbf{a}_2)$ are their orientational distribution functions averaged along with the chain contour. The last term σ in eq 2.3 is the conformational entropy loss due to the orientation of tangent vectors $\mathbf{a}$, which is also expressed in trems of $\bar{f}(\mathbf{a})$.[20] In the isotropic solution, ρ and σ are equal to unity and zero, respectively.

Table 1. Parameters Appearing in the Barker−Henderson Theory[19]

i	$P^{(i)}$	$Q^{(i)}$	$C^{(i)}$	$\alpha^{(i)}$	$\beta^{(i)}$
1	−4.97419	0.487962	1.700943	1.5	$\sqrt{2}$
2		−3.98844	−3.19927	2.75	$\sqrt{2}$

Barker and Henderson[19] calculated the first and second-order perturbation terms in ΔF for spheres with the hard core of the diameter d and the square-well potential of the depth ϵ and the width $d/2$, by a Monte Carlo simulation, and obtained the higher order perturbation terms using the Padé approximation. Their result can be written as

$$\Delta F_{w,sphere} = n\Psi(\epsilon)d^3c', \quad \Psi(\epsilon) \equiv \frac{P^{(1)}f^{(1)^2}\epsilon}{f^{(1)}k_BT - (1/2)f^{(2)}\epsilon} \quad (2.6)$$

where $f^{(1)}$ and $f^{(2)}$ are functions related to the first and second-order perturbations, respectively, given by

$$f^{(i)} = 1 + Q^{(i)}c'^* + \frac{C^{(i)}}{c'^*}\left[1 - \exp\left(-\frac{\alpha^{(i)}c'^*}{\beta^{(i)} - c'^*}\right)\right] - \frac{\alpha^{(i)}C^{(i)}}{\beta^{(i)}} \quad (i = 1, 2) \quad (2.7)$$

Here, c'^* is the reduced number concentration, defined by $(6/\pi)vc'$, and the parameters $Q^{(i)}$, $C^{(i)}$, $\alpha^{(i)}$, and $\beta^{(i)}$, as well as $P^{(1)}$ in eq 2.7, are given in Table 1.

By using the decoupling approximation of Parsons,[21] we may extend the Barker−Henderson theory to the spherocylinder system. As explained in Appendix, the final results of the perturbation terms $\Delta F_{w,mm}$, $\Delta F_{w,me}$, and $\Delta F_{w,ee}$ read

$$\Delta F_{w,mm} = nb_{mm}\Psi(\epsilon_{mm})c', \quad \Delta F_{w,me} = nb_{me}\Psi(\epsilon_{me})c', \quad \Delta F_{w,ee} = nb_{ee}\Psi(\epsilon_{ee})c' \quad (2.8)$$

where ϵ_{mm}, ϵ_{me}, and ϵ_{ee} are depths of the attractive potentials $w_{mm}(r)$, $w_{me}(r)$, and $w_{ee}(r)$, respectively, and b_{mm}, b_{me}, and b_{ee} are defined by

$$b_{mm} \equiv \frac{3{L_c}^2 d\rho}{8}, \quad b_{me} \equiv \frac{3L_cd^2}{4}, \quad b_{ee} \equiv d^3 \quad (2.9)$$

The reciprocal of the osmotic compressibility $\partial\Pi/\partial c$ can be calculated from ΔF given by eq 2.2 as

$$\frac{\partial\Pi}{\partial c} = \frac{\partial\Pi_0}{\partial c} + \frac{\partial\Pi_{w,mm}}{\partial c} + \frac{\partial\Pi_{w,me}}{\partial c} + \frac{\partial\Pi_{w,ee}}{\partial c} \quad (2.10)$$

where

$$\frac{\partial\Pi_0}{\partial c} = \frac{RT}{M(1-vc')^2}\left[1 + B\frac{c'}{1-vc'} + C\left(\frac{c'}{1-vc'}\right)^2\right] \quad (2.11)$$

and

$$\frac{\partial \Pi_{w,X}}{\partial c} = \frac{2RTM_L}{3d^2M^2} b_X \left[2\Psi(\epsilon_X) c'^* + 4 \frac{d\Psi(\epsilon_X)}{dc'^*} c'^{*2} + \frac{d^2\Psi(\epsilon_X)}{dc'^{*2}} c'^{*3} \right] \quad (X = \mathrm{mm, me, ee}) \quad (2.12)$$

Here, M_L and M are the molar mass per unit contour length and the molecular weight of the chain, respectively. Furthermore, from the virial expansion of $\partial\Pi/\partial c$, we obtain[11]

$$A_2 = \frac{\pi d N_A}{4M_L^2} \left[1 + \frac{\delta}{d} + \left(\frac{8}{3} + \frac{\delta'}{d} \right) \frac{dM_L}{M} + \left(\frac{4}{9} + \frac{\delta''}{d} \right) \left(\frac{dM_L}{M} \right)^2 \right] \quad (2.13)$$

and

$$A_3 = \frac{5\pi^2 d^3 N_A^2}{24 M_L^3} \left[1 + \frac{\delta^3}{d} + \left(\frac{17}{10} + \frac{\delta_3'}{d} \right) \frac{dM_L}{M} + \left(\frac{2}{5} + \frac{\delta_3''}{d} \right) \left(\frac{dM_L}{M} \right)^2 + \frac{2}{135} \left(\frac{dM_L}{M} \right)^3 \right] \quad (2.14)$$

where N_A is the Avogadro constant and

$$\frac{\delta}{d} = \frac{3P^{(1)}\epsilon_{mm}\rho}{\pi(2k_BT - \epsilon_{mm})} \quad (2.15)$$

$$\frac{\delta'}{d} = -\frac{2P^{(1)}}{\pi} \left(\frac{2\epsilon_{mm}\rho}{2k_BT - \epsilon_{mm}} - \frac{3\epsilon_{me}}{2k_BT - \epsilon_{me}} \right) \quad (2.16)$$

$$\frac{\delta''}{d} = \frac{4P^{(1)}}{3\pi} \left(\frac{\epsilon_{mm}\rho}{2k_BT - \epsilon_{mm}} - \frac{3\epsilon_{me}}{2k_BT - \epsilon_{me}} + \frac{6\epsilon_{ee}}{2k_BT - \epsilon_{ee}} \right) \quad (2.17)$$

$$\frac{\delta_3}{d} = \frac{54P^{(1)}\rho}{5\pi^2} \frac{2k_BTY^{(1)}\epsilon_{mm} - (2Y^{(1)} - Y^{(2)})\epsilon_{mm}^2}{(2k_BT - \epsilon_{mm})^2} \quad (2.18)$$

$$\frac{\delta_3'}{d} = \frac{108P^{(1)}}{5\pi^2} \frac{2k_BTY^{(1)}\epsilon_{me} - (2Y^{(1)} - Y^{(2)})\epsilon_{me}^2}{(2k_BT - \epsilon_{me})^2} - \frac{4\delta_3}{3d} \quad (2.19)$$

$$\frac{\delta_3''}{d} = \frac{144P^{(1)}}{5\pi^2} \frac{2k_BTY^{(1)}\epsilon_{ee} - (2Y^{(1)} - Y^{(2)})\epsilon_{ee}^2}{(2k_BT - \epsilon_{ee})^2} - \frac{4\delta_3}{9d} - \frac{2\delta_3'}{3d} \quad (2.20)$$

with $Y^{(i)}$ being defined as

$$Y^{(i)} \equiv \frac{\alpha^{(i)}C^{(i)}}{\beta^{(i)2}} \left(1 - \frac{\alpha^{(i)}}{2} \right) + Q^{(i)} \quad (2.21)$$

Inclusion of Multiple-Contact Effects on A_2 and A_3. Considering the effects of multiple-contacts and chain-ends, Yamakawa[22] calculated A_2 on the basis of the helical wormlike chain model bearing beads along the chain contour. His result is written as

$$A_2 = A_2^{(HW)} + A_2^{(E)} \quad (2.22)$$

where $A_2^{(HW)}$ is A_2 of the helical wormlike chain without the effect of chain ends, and $A_2^{(E)}$ considers the chain-end effect. The former is given by

$$A_2^{(HW)} = \frac{N_A c_\infty^{3/2} B}{2M_L^2} h(\hat{z}) \quad (2.23)$$

where c_∞ and B are the characteristic ratio and the excluded-volume strength, respectively. For the helical wormlike chain with the stiffness parameter λ^{-1} and the curvature κ_0 and torsion τ_0 of the characteristic helix, c_∞ is given by[6]

$$c_\infty = \frac{4 + (\tau_0/\lambda)^2}{4 + (\kappa_0/\lambda)^2 + (\tau_0/\lambda)^2} \quad (2.24)$$

The function $h(\hat{z})$ in eq 2.23 takes the multiple-contact effect into account, and the argument $\hat{z}$ is an excluded-volume parameter including the chain stiffness effect. Yamakawa[22] proposed to express $h(\hat{z})$ as

$$h(\hat{z}) = (1 + 7.74\hat{z} + 52.3\hat{z}^{27/10})^{-10/27} \quad (2.25)$$

and $\hat{z}$ as

$$\hat{z} = \frac{Q(N)}{2.865} \left(\frac{3}{2\pi\alpha_S^2} \right)^{3/2} B N^{1/2} \quad (2.26)$$

where $N \equiv \lambda M/M_L$, the function $Q(N)$ of N is the coefficient of the double-contact term in the $h(\hat{z})$ function, and α_S is the radius expansion factor due to the intramolecular excluded volume effect, which is a function of B and N.[22] The explicit functional form of $Q(N)$ for $N \gtrsim 1$ is given in ref 23.[24]

The chain-end effect term $A_2^{(E)}$ in eq 2.22 is written in the form[22]

$$A_2^{(E)} = \frac{a_{2,1}}{M} + \frac{a_{2,2}}{M^2} \quad (2.27)$$

where $a_{2,1}$ and $a_{2,2}$ are parameters characterizing interchain interactions between the chain middle and end portions and between two chain-end portions, respectively. Equation 2.27, which was derived using the single-contact approximation, is compared with eq 2.13 to obtain the relations

$$a_{2,1} = \frac{\pi d^2 N_A}{4M_L} \left(\frac{8}{3} + \frac{\delta'}{d} \right), \quad a_{2,2} = \frac{\pi d^3 N_A}{4} \left(\frac{4}{9} + \frac{\delta''}{d} \right) \quad (2.28)$$

In a similar method, but including the effect of the three-body interaction,[25] A_3 can be calculated as[6]

$$A_3 = \frac{N_A^2 c_\infty^3}{3M_L^3} \left[B_3 + \frac{3M}{4M_L} B^2 h^2(\hat{z}) g_2(\hat{z}') \right] + \frac{a_{3,1}}{M} + \frac{a_{3,2}}{M^2} + \frac{a_{3,3}}{M^3} \quad (2.29)$$

where B_3 is the strength of the three-body interaction and the function $g_2(\hat{z}')$ of an excluded-volume parameter $\hat{z}'$ considers the multiple-contact effect on the reduced third virial coefficient (within the binary cluster ap-

proximation). Norisuye et al.[26] proposed to calculate $g_2(\hat{z}')$ and $\hat{z}'$ by

$$g_2(\hat{z}') = \frac{2.219\hat{z}'}{(1 + 18\hat{z}' + 12.6\hat{z}'^2)^{1/2}} \tag{2.30}$$

and

$$\hat{z}' = \frac{U(N)}{2.219}\left(\frac{3}{2\pi\alpha_S^2}\right)^{3/2} BN^{1/2} \tag{2.31}$$

with the coefficient $U(N)$ of the double-contact term in the $g_2(\hat{z}')$ function, which is given in ref 26 for $N \gtrsim 3$;[24] in the original paper, $U(N)$ is denoted as C. The second to fourth terms in eq 2.29 take into account the effects of chain ends on A_3 up to single-contact terms, and comparing those terms with eq 2.14, we have the following relations:

$$a_{3,1} = \frac{5\pi^2 d^4 N_A^2}{24M_L^2}\left(\frac{17}{10} + \frac{\delta_3'}{d}\right), \quad a_{3,2} = \frac{5\pi^2 d^5 N_A^2}{24M_L}\left(\frac{2}{5} + \frac{\delta_3''}{d}\right),$$
$$a_{3,3} = \frac{\pi^2 d^6 N_A^2}{324} \tag{2.32}$$

In general, $\partial\Pi/\partial c$ (or Π) must be also expressed in a terms of the excluded-volume parameter z. However, at present, we have no available expression of $\partial\Pi/\partial c$ as a function of z. In what follows, we use eq 2.10 for $\partial\Pi/\partial c$, based on the single-contact approximation and free from z, which is applicable only to polymer solutions with sufficiently small N.

3. Experimental Section

Samples. Standard polystyrene (oligostyrne) samples F-1, A-5000, A-2500, A-1000, and A-500, purchased from Tosoh Co. Ltd., were divided into several fractions by fractional precipitation using toluene as the solvent and methanol as the precipitant (or using acetone as the solvent and water as the precipitant for lower molecular weight samples), and each middle fraction was used for sedimentation equilibrium experiment. In what follows, the original sample codes were used for the middle fractions used.

Sedimentation Equilibrium. Dilute through concentrated toluene solutions of polystyrene samples were investigated by sedimentation equilibrium, using a Beckman-Coulter Optima XL-I ultracentrifuge, equipped with a Rayleigh interferometer with a 675-nm light emitting from a diode laser. The temperature was chosen to be 15 °C, according to Yamakawa et al.[16,17] who studied the second virial coefficient A_2 for the same system over a wider molecular weight range. Aluminum 12-mm double-sector cells were used, and the height of the solution column was adjusted to ca. 2.5 mm. The apparent molecular weight M_{app} was calculated from the equation

$$M_{app} = \frac{2RT(c_b - c_a)}{\omega^2(r_b^2 - r_a^2)c_0(\partial\rho/\partial c)} \tag{3.1}$$

where r_b and r_a are the distance from the center of revolution to the cell bottom and meniscus, respectively, c_b and c_a are polymer mass concentrations at r_b and r_a, respectively, under the centrifugal field which is estimated by interferometry, ω is the angular velocity, ρ and c are the density and mass concentration of the solution, respectively, c_0 is c of the solution at $\omega = 0$, and R is the gas constant. Three different rotor speeds were chosen for each sample (except for sample A-500) in the range from 10 000 to 30 000 rpm, and the angular velocity independence of M_{app} was checked. For sample A-500, the rotor speed was chosen as 33 000 rpm.

Table 2. Characteristics of Polystyrene Samples Used

sample	$\partial\rho/\partial c$	$\partial n/\partial c$/ cm^3 g^{-1}	M_w	$A_2/10^{-3}$ cm^3 mol^{-1} g^{-2}	$A_3/10^{-3}$ cm^6 mol^{-1} g^{-3}
F-1	0.2135	0.102	9700[a] (9500)[b]	0.91[a] (1.04)[b]	4.5[a]
A-5000	0.1964	0.101_5	6100[a] (5850)[b]	1.13[a] (1.21)[b]	3.65[a]
A-2500	0.1858	0.0928	2900[a] (2700)[b]	1.58[a] (1.60)[b]	3.7[a]
A-1000	0.1670	0.0848	1150[a] (1050)[b]	2.50[a] (2.65)[b]	4.2*a*
A-500	0.1399	0.0710	(550)[b]	(3.80)[b]	

[a] Determined from the Bawn plot. [b] Determined from the square-root plot.

If the concentration difference $\Delta c \equiv c_b - c_a$ is much smaller than the average concentration $\bar{c} \equiv (c_b + c_a)/2$, M_{app} is related to the reciprocal of the osmotic compressibility $\partial\Pi/\partial c$ at $c = \bar{c}$ by[27,28]

$$\frac{1}{M_{app}} = \frac{1}{RT}\frac{\partial\Pi}{\partial c} \tag{3.2}$$

The rotor speed chosen in this study was so low that $\Delta c/\bar{c}$ is less than 0.3 and the above relation is available but still high enough for the fringe displacement between r_a and r_b to be larger than three fringes, to guarantee experimental accuracy in Δc or M_{app}. For dilute solutions, eq 3.2 gives us[27-29]

$$\frac{1}{M_{app}} = \frac{1}{M_w} + 2A_2\bar{c} + 3A_3\bar{c}^2 + O(\bar{c}^3) \tag{3.3}$$

where M_w is the weight-average molecular weight and A_2 and A_3 are the second and third virial coefficient, respectively.

Densitometry and Refractometry. Densities ρ and excess refractive indices Δn of toluene solutions of all polystyrene samples were measured at 15 °C as functions of the polymer concentration c to obtain $\partial\rho/\partial c$ and $\partial n/\partial c$ (at constant pressure), which are necessary to calculate M_{app}. While the former measurement was made with an oscillation U-tube densitometer (Anton-Paar, DMA5000), the latter measurement was performed with a differential refractometer (Ohtsuka Electronics, DRM-1020) at 675 nm for dilute solutions and with a modified Schultz−Cantow type differential refractometer with a mercury lamp at 436 and 546 nm for concentrated solutions; the results of Δn for concentrated solutions were extrapolated to the wavelength of 675 nm using Couchy dispersion formula. The results of $\partial\rho/\partial c$ and $\partial n/\partial c$ for each sample are listed in Table 2. Both $\partial\rho/\partial c$ and $\partial n/\partial c$ almost linearly depended on the reciprocal of the molecular weight (see below for the molecular weight determination) but did not depend on c up to ca. 0.3 g/cm^3 within experimental errors.

4. Results and Discussion

Molecular Weights and Second and Third Virial Coefficients. Figure 1 shows the plot of $M_{app}^{-1/2}$ vs $\bar{c}$ (the square-root plot) for dilute toluene solutions of five low molecular weight polystyrene samples at 15 °C. The linearity of this plot maintains up to higher $\bar{c}$ than the linear plot (i.e., the plot of M_{app}^{-1} vs $\bar{c}$) as in the case of the Berry plot for light scattering experiments.[17] From the intercept and initial slope, we have determined M_w and A_2 for each sample, using eq 3.3. The results are listed in the parentheses of the fourth and fifth columns of Table 2.

For light scattering and osmometry, experimental data were sometimes analyzed by so-called the Bawn plot[5,30,31] to estimate M_w, A_2, and A_3 accurately. Now we apply this plot to the sedimentation equilibrium data. Numbering the experimental data of sedimentation equilibrium for different concentrations as $i = 1$, 2, ... and denoting the average concentration and apparent molecular weight of the ith datum as $\bar{c}_i$ and

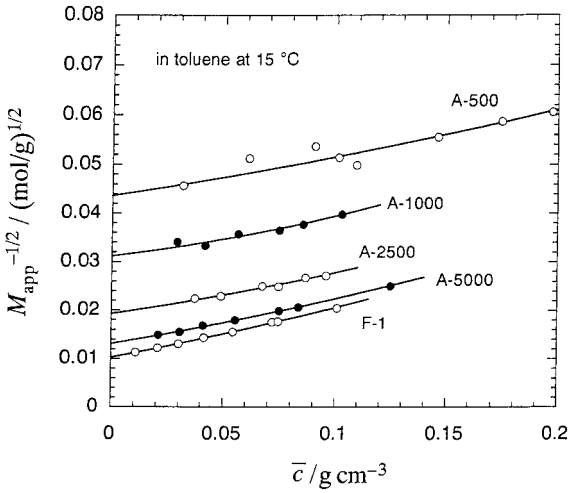

Figure 1. Plots of $M_{app}^{-1/2}$ vs $\bar{c}$ for dilute toluene solutions of five polystyrene samples at 15 °C.

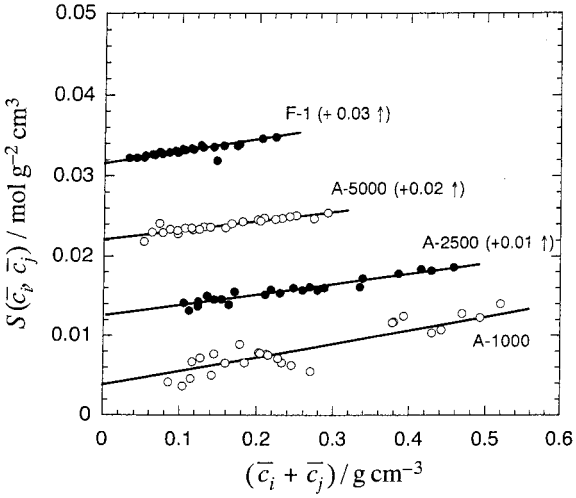

Figure 2. Bawn plot for toluene solutions of four polystyrene samples at 15 °C.

$M_{app}(\bar{c}_i)$, respectively, we obtain the following equation from eq 3.3:

$$S(\bar{c}_i,\bar{c}_j) \equiv \frac{M_{app}(\bar{c}_j)^{-1} - M_{app}(\bar{c}_i)^{-1}}{\bar{c}_j - \bar{c}_i} = 2A_2 + 3A_3(\bar{c}_i + \bar{c}_j) + \ldots \quad (4.1)$$

Figure 2 shows the plot of $S(\bar{c}_i,\bar{c}_j)$ against $\bar{c}_i + \bar{c}_j$ for four polystyrene samples. Although the data points are slightly scattered especially for sample A-1000, we have determined A_2 and A_3 for each sample from eq 4.1 with the line drawn in the figure. The value of M_w was also re-estimated by the extrapolation of the quantity $M_{app}^{-1} - (2A_2\bar{c} + 3A_3\bar{c}^2)$ calculated with A_2 and A_3 determined by the Bawn plot, to zero concentration. The results are listed in the fourth to sixth columns of Table 2. Relative differences in A_2 and M_w determined from the Bawn and square-root plots are within ca. 10%. For the lowest molecular weight sample A-500, data points in the Bawn plot were too scattered to determine A_2 and A_3.

In Figure 3, our results (filled circles) of A_2 in 15 °C toluene obtained above from the Bawn plot (for the lowest M_w sample from the square-root plot) are compared with Yamakawa et al.'s results[16,17] (unfilled circles) under the same solvent conditions over a wider

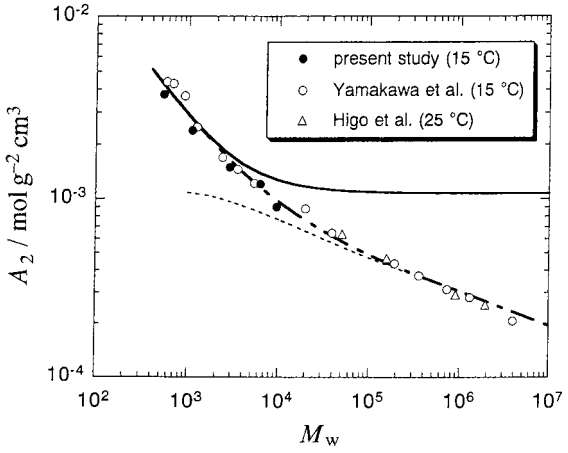

Figure 3. Molecular weight dependence of A_2 in toluene. Key: filled circles, data obtained in the present study (at 15 °C); unfilled circles, data of Yamakawa et al.[16,17] (at 15 °C); triangles, data of Higo et al.[14] (at 25 °C); solid curve, A_2 calculated by eq 2.13; dashed curve, $A_2^{(HW)}$ calculated by eq 2.23 with $B = 0.74$ nm; dot−dashed curve, A_2 calculated by the Yamakawa theory (eqs 2.22, 2.23, and 2.27) with $a_{2,1} = 2.0$ cm^3/g and $a_{2,2} = -150$ cm^3/mol.

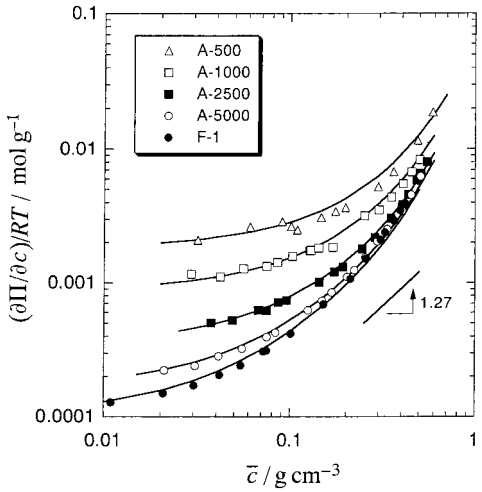

Figure 4. Double logarithmic plot of $(\partial\Pi/\partial c)/RT$ vs $\bar{c}$ for toluene solutions of low molecular weight polystyrene samples at 15 °C. Solid curves: calculated by eqs 2.10−2.12 with parameters listed in Table 3.

molecular weight range, obtained by light scattering using the square-root plot. Both data points almost follow a single curve. In addition, Figure 3 contains Higo et al.'s A_2 results[14] for polystyrene in 25 °C toluene (triangles), obtained by osmometry using the square-root plot, which also follow the same curve.

Yamakawa et al. demonstrated that their A_2 results are well explained by the theory of Yamakawa[22] given by eq 2.22 in section 2. With choosing the excluded-volume strength B in $A_2^{(HW)}$ given by eq 2.23 to be 0.54 nm, which was determined from radius of gyration data, they estimated parameters $a_{2,1}$ and $a_{2,2}$ characterizing interchain interactions between the chain middle and end portions and between two chain-end portions to be 2.5 cm^3/g and −200 cm^3/mol, respectively. The chain-end effect on A_2 was found to be appreciable even at $M_w \sim 10^5$.

Osmotic Compressibility up to High Concentrations. Figure 4 shows the double logarithmic plot of $(\partial\Pi/\partial c)/RT$ vs $\bar{c}$ for toluene solutions of low molecular weight polystyrene samples at 15 °C over a wide range of the

Table 3. Molecular Parameters Used for Calculations of A_2, A_3, and $\partial\Pi/\partial c$

$\lambda^{-1} = 2.06$ nm[6]	$d = 0.56$ nm	$B_3 = 1.4$ nm^3
$\kappa_0 = 3.0$ nm^{-1} [6]	$\delta = -0.27$ nm	$\delta_3 = -0.15$ nm
$\tau_0 = 6.0$ nm^{-1} [6]	$\delta' = 1.2$ nm	$\delta_3' = 1.6$ nm
$M_L = 358$ nm^{-1} [6]	$\delta'' = -1.3$ nm	$\delta_3'' = -2.2$ nm
$B = 0.74$ nm	ϵ_{mm}/k_BT [a] $= 0.18$	
$a_{2,1} = 2.0$ cm^3/g	ϵ_{me}/k_BT [a] $= -0.38$	
$a_{2,2} = -150$ cm^6/mol	ϵ_{ee}/k_BT [a] $= 0.15$	

[a] $\epsilon_{mm}/k_BT = 2\pi\delta/(3P^{(1)}d\rho + \pi\delta)$, $\epsilon_{me}/k_BT = 2\pi(4\delta + 3\delta')/[18P^{(1)}d + \pi(4\delta + 3\delta')]$, $\epsilon_{ee}/k_BT = 2\pi(4\delta + 6\delta' + 9\delta'')/[72P^{(1)}d + \pi(4\delta + 6\delta' + 9\delta'')]$.

concentration. Data points for each sample obey a curve convex downward, and the scaling law does not hold for such low molecular weight polystyrene samples. Higo et al.[14] found that osmotic pressure for semidilute toluene solutions of higher molecular weight polystyrenes (at 25 °C) obeys the scaling law proposed by des Cloizeaux.[32,33] The slope of the segment in Figure 4 indicates the exponent of this scaling law for $\partial\Pi/\partial c$. The concentration dependence for the low molecular weight samples is stronger than this scaling law at higher concentrations. It is seen from Figure 4 that the molecular weight dependence of $(\partial\Pi/\partial c)/RT$ becomes weaker with increasing the polymer concentration.

Determination of Interaction Parameters. Here we use a spherocylinder model bearing hard core and square-well potentials to characterize the intermolecular interaction of polystyrene in toluene. To incorporate the chain-end effect, the middle cylinder and end hemisphere of the spherocylinder model are assumed to possess different interaction nature, i.e., depths of the square-well potential between two cylinders (ϵ_{mm}), between the cylinder and hemisphere (ϵ_{me}), and between two hemispheres (ϵ_{ee}) are differentiated. The hard-core diameter of the spherocylinder is represented by d, and the width of the square-well potential is assumed to be $d/2$, according to Barker and Henderson[19] (cf. section 2). The four interaction parameters d, ϵ_{mm}, ϵ_{me}, and ϵ_{ee} can be determined from experimental results of A_2 and $\partial\Pi/\partial c$ as explained below.

Before doing this task, we analyze A_2 data by the Yamakawa theory[22] based on the helical wormlike chain model bearing beads along the chain contour. In a sufficiently high molecular weight region, the end-effect term $A_2^{(E)}$ is negligible in comparison with $A_2^{(HW)}$ in eq 2.22. If one chooses the excluded-volume strength $B =$ 0.74 nm, $A_2^{(HW)}$ calculated by eq 2.23 (the dashed curve in Figure 3) fits experimental A_2 at $M_w \gtrsim 10^5$. In the calculation, we have used the helical wormlike chain parameters λ^{-1}, κ_0, τ_0, and M_L listed in Table 3, which were determined by Yamakawa et al.[6,34] The value of B is slightly larger than that (=0.54 nm) determined from radius of gyration data.[6,34]

According to Einaga et al.,[17] we estimate $A_2^{(E)}$ in a low M_w region by subtracting theoretical $A_2^{(HW)}$ from experimental A_2 obtained in this study and also by Yamakawa et al.,[16,17] to plot $A_2^{(E)}M_w$ against M_w^{-1} (cf. Figure 5). Although the data points are rather scattered, we have determined the chain-end effect parameters $a_{2,1}$ and $a_{2,2}$ to be 2.0 cm^3/g and -150 cm^3/mol, respectively, from the intercept and slope of the plot. The results are not so much different from those estimated by Einaga et al.[17] with $B = 0.54$ nm. The dot−dashed curve in Figure 3 indicates A_2 calculated by the Yamakawa theory with the parameters determined above. The agreement between the theory and experiment is satisfactory.

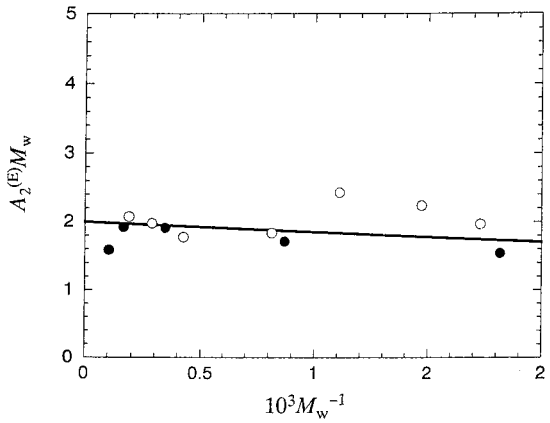

Figure 5. Plots of $A_2^{(E)}M_w$ against M_w^{-1} constructed using A_2 data at $M_w < 10^4$. Key: filled circles, data obtained in the present study; unfilled circles, data of Yamakawa et al.[16,17]

While the Yamakawa theory takes into account the multiple-contact effect on A_2, the theory based on the spherocylinder model, explained in section 2 (cf. eq 2.13), considers only the single-contact term in A_2. Since multiple-contact terms in A_2 should be negligible at sufficiently low molecular weights, A_2 for the spherocylinder model, calculated by eq 2.13, is required to approach to that of the Yamakawa theory with decreasing the molecular weight. With this requirement, we can determine the parameter $d + \delta$ of the spherocylinder, where δ is an attractive interaction parameter related to ϵ_{mm} by eq 2.15. As shown by the solid curve in Figure 3, the agreement in the low molecular weight region is obtained when $d + \delta = 0.29$ nm.[35] Here we have calculated end effect terms in eq 2.13 from $a_{2,1}$ and $a_{2,2}$ determined above. The solid curve however starts deviating from the dot−dashed curve at M_w as low as few thousands, which indicates the significance of the multiple-contact terms in A_2.

If a value of d is given, the interaction parameters ϵ_{mm}, ϵ_{me}, and ϵ_{ee} can be calculated from the values of $d + \delta$, $a_{2,1}$, and $a_{2,2}$ determined above by using eqs 2.15−2.17 and 2.28, and then $\partial\Pi/\partial c$ can be estimated by eqs 2.10−2.12. A trial-and-error method was used to find a d value which leads to the closest agreement between theoretical and experimental $\partial\Pi/\partial c$. It is shown by solid curves in Figure 4 that the theory with $d = 0.56$ nm gives best fit to the data points for polystyrene with $M_w < 10^4$. The parameters ϵ_{mm}, ϵ_{me}, and ϵ_{ee} calculated with $d = 0.56$ nm are listed in Table 3. The depth ϵ_{mm} of the square-well potential is much less than the thermal energy k_BT, as expected in the good solvent toluene. Only ϵ_{me} is negative, i.e., the dispersion interaction between the middle and end portions of polystyrene is repulsive. This is not unreasonable if the chemical structure of the terminal group is different from that of the monomer unit in the polystyrene chain.[36]

With the single-contact approximation, the third virial coefficient A_3 can be calculated by eq 2.14 with eqs 2.18−2.20, where all the parameters included have been already determined. In Figure 6, the theoretical results (the solid curve) are compared with our experimental results (the circles). While the lowest-molecular-weight data point is on the solid curve, the multiple-contact effect becomes appreciable with increasing M_w, as in the case of A_2 shown in Figure 3. This effect on A_3 is included in eq 2.29, where B_3 remains as the unknown parameter.[25] If one chooses a value of 1.4 nm^3 for this parameter, theoretical results (the dot−dashed curve in

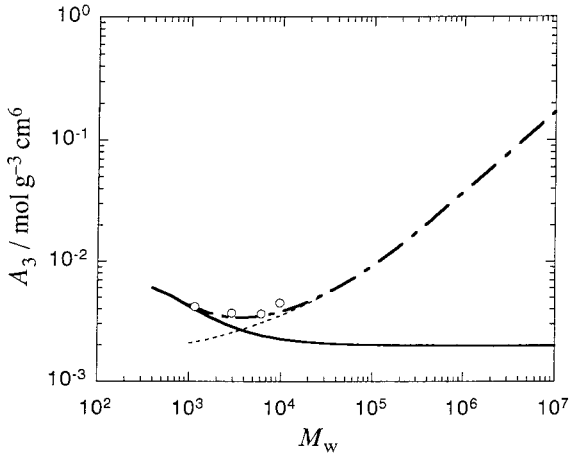

Figure 6. Comparison of experimental A_3 with theoretical ones calculated by eq 2.14 (solid curve), by eq 2.29 with $B_3 = 1.4$ nm^3 and $a_{3,1}$, $a_{3,2}$, and $a_{3,3}$ estimated by eqs 2.32 (dot−dashed curve), and by eq 2.29 with $B_3 = 1.4$ nm^3 and $a_{3,1} = a_{3,2} = a_{3,3} = 0$ (dashed curve).

Figure 6) calculated by eq 2.29 asymptotically coincide with those of eq 2.14 in the low molecular weight region. (The parameters $a_{3,1}$, $a_{3,2}$, and $a_{3,3}$ in eq 2.29 were estimated by eq 2.32 with δ_3' and δ_3'' being calculated by eqs 2.19 and 2.20; cf. Table 3.) The experimental results follow the dot−dashed curve as expected. The value of B_3 chosen is considerably larger than that (=0.28 nm^3) reported for polystyrene in 34.5 °C cyclohexane.[6,37] In Figure 6, the dashed curve indicates theoretical A_3 without the chain-end effect, calculated eq 2.29 with $a_{3,1} = a_{3,2} = a_{3,3} = 0$. It is seen that the chain-end effect becomes appreciable at $M_w \lesssim 2 \times 10^4$, being less important in A_3 than in A_2 (cf. Figure 3).

On the Single-Contact Approximation. From Figures 3 and 6, it turns out that the multiple-contact effect becomes appreciable for A_2 and A_3 at M_w higher than few thousands. On the other hand, the theory for $\partial\Pi/\partial c$ based on the single-contact approximation can fit experimental data up to $M_w \sim 10^4$, as shown in Figure 4. The wider applicability of the single-contact approximation for $\partial\Pi/\partial c$ may be owing to the cancellation of multiple-contact terms in all virial terms. It is noted that the multiple-contact effects in the second and third virial terms alter $\partial\Pi/\partial c$ in the opposite direction, as seen in Figures 3 and 6.

Noda et al.[10,14] measured osmotic pressures Π for toluene solutions of four polystyrene samples (PS-1−PS-4) with molecular weights higher than 5×10^4 at 25 °C over wide ranges of concentration. Fitting their results to suitable functions of c, and differentiating the functions with respect to c, we obtained $\partial\Pi/\partial c$ for their samples. Furthermore, Scholte[13] a long time ago made sedimentation equilibrium measurements for toluene solutions of a polystyrene sample with $M_w = 1.63 \times 10^5$ over a wide concentration range (at 25 °C). Figure 7 compares those data of $(\partial\Pi/\partial c)/RT$ for $M_w > 5 \times 10^4$ (along with our data for sample F-1) with the theoretical results calculated by eq 2.10 with the interaction parameters determined above from $\partial\Pi/\partial c$ data for our lower molecular weight samples (cf. Table 3). With increasing molecular weight, the theory tends to overestimate experimental $\partial\Pi/\partial c$ at $c \lesssim 0.1$ g/cm^3, demonstrating the importance of the multiple-contact effect on $\partial\Pi/\partial c$ for higher molecular weight polystyrenes. The upper limit of the molecular weight for the applicability

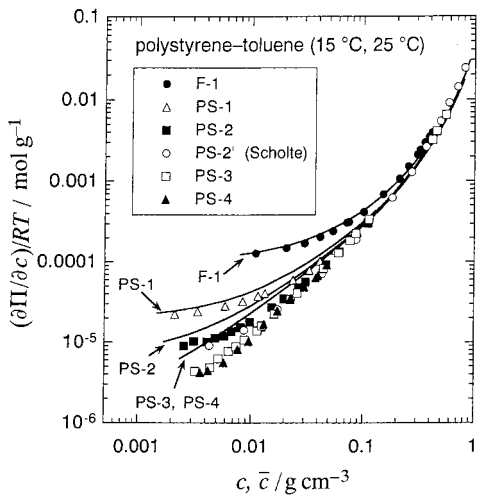

Figure 7. Comparison of $(\partial\Pi/\partial c)/RT$ for 25 °C toluene solutions of polystyrenes with the molecular weight higher than 10^4 with theoretical ones calculated by eqs 2.10−2.12 with the same interaction parameters as used in Figure 4. Data points, obtained in the present study (F-1, $M_w = 0.97 \times 10^4$), by Noda et al.[10,14] (PS-1, $M_n = 5.1 \times 10^4$; PS-2, $M_n = 1.57 \times 10^5$; PS-3, $M_w = 9.0_1 \times 10^5$; PS-4, $M_w = 1.9_3 \times 10^6$) and by Scholte[13] (PS-2′, $M_w = 1.63 \times 10^5$), where M_n is the number-average molecular weight.

of the single-contact approximation to $\partial\Pi/\partial c$ is between 1×10^4 and 5×10^4.

It is seen from Figure 7 that the single-contact approximation becomes good at $c \gtrsim 0.1$ g/cm^3 even for high molecular weight samples. In particular, for the samples with $M_w = 1.63 \times 10^5$ and 9×10^5, the agreement between theory and experiment maintains up to very high c. The concentration 0.1 g/cm^3 is close to the crossover between the semidilute and concentrated regions for polystyrene in toluene as reported by Noda et al.[10] We may say that the multiple-contact effect on thermodynamic properties for flexible polymer solutions is screened off in the concentrated region.

Acknowledgment. We are grateful to Prof. Takashi Norisuye at Osaka University for valuable comments about the second and third virial coefficients.

Appendix. Decoupling Approximation of Parsons[21,38]

Parsons[21] formulated the free energy ΔF of the system of rodlike molecules on the basis of thermodynamic functions of spherical molecules. Instead of the $u(r)$ given by eq 2.1, he used the intermolecular interaction $u(\mathbf{R},\mathbf{a}_1,\mathbf{a}_2)$ between rods 1 and 2 as a function of the vector $\mathbf{R}$ between their centers of mass and their unit orientation vectors $\mathbf{a}_1$ and $\mathbf{a}_2$, and formally expressed ΔF by[18]

$$\frac{\Delta F}{nk_BT} = -\frac{1}{6k_BT}\int_0^{c'} dc'' \int d\mathbf{a}_1\, d\mathbf{a}_2\, f(\mathbf{a}_1) f(\mathbf{a}_2) \int d\mathbf{R} \times [\mathbf{R}\cdot\nabla u(\mathbf{R},\mathbf{a}_1,\mathbf{a}_2)] g(\mathbf{R},\mathbf{a}_1,\mathbf{a}_2;c'') + \sigma \quad \text{(A1)}$$

where the operator ∇ acts only on the $\mathbf{R}$ coordinate of u and where g is the radial distribution function.

If the multivariate functions $u(\mathbf{R},\mathbf{a}_1,\mathbf{a}_2)$ and $g(\mathbf{R},\mathbf{a}_1,\mathbf{a}_2)$ are approximated by functions $\hat{u}(R/\tau)$ and $\hat{g}(R/\tau)$ of the single variable R/τ, where $R = |\mathbf{R}|$ and τ is some range parameter depending on $\mathbf{e}_R$ (the unit vector parallel to

R), $\mathbf{a}_1$, and $\mathbf{a}_2$, eq A1 can be simplified by

$$\frac{\Delta F}{nk_BT} \cong -\frac{1}{6k_BT}\int_0^{c'} dc'' \int_0^{\infty} dy y^3 \frac{\partial \hat{u}}{\partial y}\hat{g}(y;c'') \times \int d\mathbf{a}_1\, d\mathbf{a}_2\, f(\mathbf{a}_1)f(\mathbf{a}_2)\int d\mathbf{e}_R \tau^3(\mathbf{e}_R,\mathbf{a}_1,\mathbf{a}_2) + \sigma$$
$$\cong -\frac{1}{2k_BT}[\alpha_0(c') + \alpha_w(c')]\int d\mathbf{a}_1\, d\mathbf{a}_2\, f(\mathbf{a}_1)f(\mathbf{a}_2)V_{excl} + \sigma \quad \text{(A2)}$$

where

$$\alpha_0(c') \equiv \int_0^{c'} dc'' \int_0^{\infty} dy y^3 \frac{\partial \hat{u}_0}{\partial y}\hat{g}(y;c''),$$
$$\alpha_w(c') \equiv \int_0^{c'} dc'' \int_0^{\infty} dy y^3 \frac{\partial \hat{w}}{\partial y}\hat{g}(y;c'') \quad \text{(A3)}$$

and V_{excl} is the excluded volume between two rods due to the core-potential. Equation A2 decouples the translational and orientational degrees of freedom, and is just the same as ΔF for the system of spherical molecules where $y \equiv R/d$ (d: the diameter of the sphere) and $V_{excl} = (4/3)\pi d^3$. Identifying the attractive part of this equation for spherical molecules with $\Delta F_{w,sphere}$ given by eq 2.6, we can express $\alpha_w(c')$ in terms of $\Psi(\epsilon)$, and inserting the resulting expression of $\alpha_w(c')$ into eq A2, we obtain eqs 2.8 with eqs 2.9.

Supporting Information Available: Table 4, giving numerical results of $\partial\Pi/\partial c$ for toluene solutions of our polystyrene samples (at 15 °C). This material is available free of charges via the Internet at http://pubs.acs.org.

References and Notes

(1) de Gennes, P.-G. *Scaling Concepts in Polymer Physics*; Cornell University Press: Ithaca, NY, 1979.
(2) Doi, M.; Edwards, S. F. *The Theory of Polymer Dynamics*; Clarendon Press: Oxford, England, 1986.
(3) Fujita, H. *Polymer Solutions*; Elsevier: Amsterdam, 1990; Vol. 9.
(4) Yamakawa, H. *Modern Theory of Polymer Solutions*; Harper & Row: New York, 1971.
(5) Norisuye, T.; Fujita, H. *Chemtracts Macromol. Chem.* **1991**, *2*, 293.
(6) Yamakawa, H. *Helical Wormlike Chains in Polymer Solutions*; Springer-Verlag: Berlin and Heidelberg, Germany, 1997.
(7) Oono, Y. *Adv. Chem. Phys.* **1985**, *61*, 301.
(8) des Cloizeaux, J.; Jannink, G. *Polymers in Solution. Their Modelling and Structure*; Clarendon Press: Oxford, England, 1990.
(9) Flory, P. J. *Principles of Polymer Chemistry*; Cornell University Press: Ithaca, NY, 1953.
(10) Noda, I.; Higo, Y.; Ueno, N.; Fujimoto, T. *Macromolecules* **1984**, *17*, 1055.
(11) Sato, T.; Jinbo, Y.; Teramoto, A. *Macromolecules* **1997**, *30*, 590.
(12) Scholte, T. G. *Eur. Polym. J.* **1970**, *6*, 1063.
(13) Scholte, T. G. *J. Polym. Sci., Part A-2* **1970**, *8*, 84.
(14) Higo, Y.; Ueno, N.; Noda, I. *Polym. J.* **1983**, *15*, 367.
(15) Wiltzius, P.; Haller, H. R.; Cannell, D. S.; Schaefer, D. W. *Phys. Rev. Lett.* **1983**, *51*, 1183.
(16) Yamakawa, H.; Abe, F.; Einaga, Y. *Macromolecules* **1993**, *26*, 1898.
(17) Einaga, Y.; Abe, F.; Yamakawa, H. *Macromolecules* **1993**, *26*, 6243.
(18) Hansen, J. P.; McDonald, I. R. *Theory of Simple Liquids*, 2nd ed.; Academic Press: London, 1986.
(19) Barker, J. A.; Henderson, D. *Rev. Mod. Phys.* **1976**, *48*, 587.
(20) Sato, T.; Teramoto, A. *Adv. Polym. Sci.* **1996**, *126*, 85.
(21) Parsons, J. D. *Phys. Rev. A* **1979**, *19*, 1225.
(22) Yamakawa, H. *Macromolecules* **1992**, *25*, 1912.
(23) Yamakawa, H.; Stockmayer, W. H. *J. Chem. Phys.* **1972**, *57*, 2843.
(24) The functional $Q(N)$ and $U(N)$ also depends on a cutoff parameter. We chose this parameter to be 0.3, according to Yamakawa.[22]
(25) The three-body interaction is included in eq 2.14 for the spherocylinder model.
(26) Norisuye, T.; Nakamura, Y.; Akasaka, K. *Macromolecules* **1993**, *26*, 3791.
(27) Fujita, H. *Foundation of Ultracentrifugal Analysis*; Wiley-Interscience: New York, 1975.
(28) Kurata, M. *Thermodynamics of Polymer Solutions*; Harwood Academic Publishers: Chur, Switzerland, 1982.
(29) Strictly, M_{app} is written as $1/M_{app} = 1/M_w + 2A_2\bar{c} + 3A_3\bar{c}^2[1 + 1/12(\Delta c/\bar{c})^2] + O(c^3)$ at low concentrations, but the error in the third term on the right-hand side of eq 3.3 is less than 1% when $\Delta c/\bar{c} = 0.3$.
(30) Bawn, C. E. H.; Freeman, R. F. J.; Kamaliddin, A. R. *Trans. Faraday Soc.* **1950**, *46*, 862.
(31) Sato, T.; Norisuye, T.; Fujita, H. *J. Polym. Sci., Part B: Polym. Phys.* **1987**, *25*, 1.
(32) des Cloizeaux, J. *J. Phys. (Paris)* **1975**, *36*, 281.
(33) des Cloizeaux, J.; Noda, I. *Macromolecules* **1982**, *15*, 1505.
(34) Abe, F.; Einaga, Y.; Yoshizaki, T.; Yamakawa, H. *Macromolecules* **1993**, *26*, 1884.
(35) As pointed out by Yamakawa and Stockmayer,[23] the single-contact term in A_2 for the cylinder model is not identical with that for the bead model. Thus we did not estimate $d + \delta$ by equating eq 2.13 to eq 2.22 with $h(\hat{z}) = 1$ at $M \rightarrow \infty$.
(36) Israelachvili, J. N. *Intermolecular and Surface Forces*, 2nd ed.; Acedemic Press: London, 1992.
(37) Nakamura, Y.; Norisuye, T.; Teramoto, A. *Macromolecules* **1991**, *24*, 4904.
(38) Vroege, G. J.; Lekkerkerker, H. N. W. *Rep. Prog. Phys.* **1992**, *55*, 1241.

MA011540Z